

Cell Reports, Volume 42

Supplemental information

**Glial progenitor heterogeneity and key regulators
revealed by single-cell RNA sequencing provide
insight to regeneration in spinal cord injury**

Haichao Wei, Xizi Wu, Joseph Withrow, Raquel Cuevas-Diaz Duran, Simranjit Singh, Lesley S. Chaboub, Jyotirmoy Rakshit, Julio Mejia, Andrew Rolfe, Juan J. Herrera, Philip J. Horner, and Jia Qian Wu

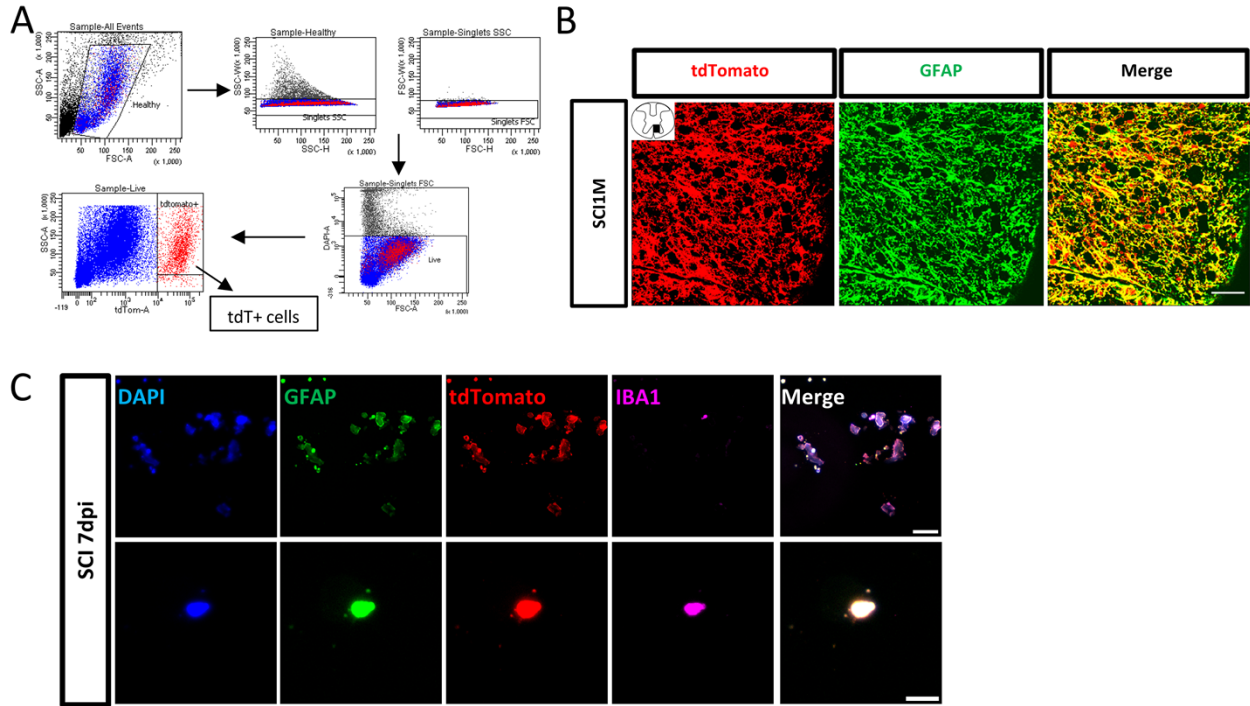


Figure S1. The isolation and validation of GFAP-expressing cells of GFAP-Cre:R26-tdT mice. Related to Figure 1. **(A)** Representative FACS workflow and gating strategy for purifying single tdT positive cells from Sham GFAP-Cre:R26-tdT spinal cord tissue at T10 segment. **(B)** Immunostaining validation of GFAP (green) and tdT (red) expression in GFAP-Cre:R26-tdT mouse spinal cord in SCI1M. Images were captured in the ventral column at 600 μm rostral from the epicenter. Scale bar, 20 μm . **(C)** Confocal images of immunostained FACS-sorted cells from 7 dpi mouse spinal cords mounted using Cytospin centrifugation and stained with DAPI, GFAP, tdT and IBA1 to confirm the quality of the FACS sorting. The top row: a representative field showing a large proportion of tdT + cells are GFAP/tdT double positive, with limited number of GFAP/tdT/IBA1 triple positive cell. Scale bar, 100 μm). The bottom row: a single cell view demonstrating the colocalization of IBA1 with both tdT and GFAP rather than doublets. Note that during cytocentrifuge preparation, cell cytoskeleton is disturbed resulting in condensed cytoplasmic staining for GFAP. Scale bar, 10 μm .

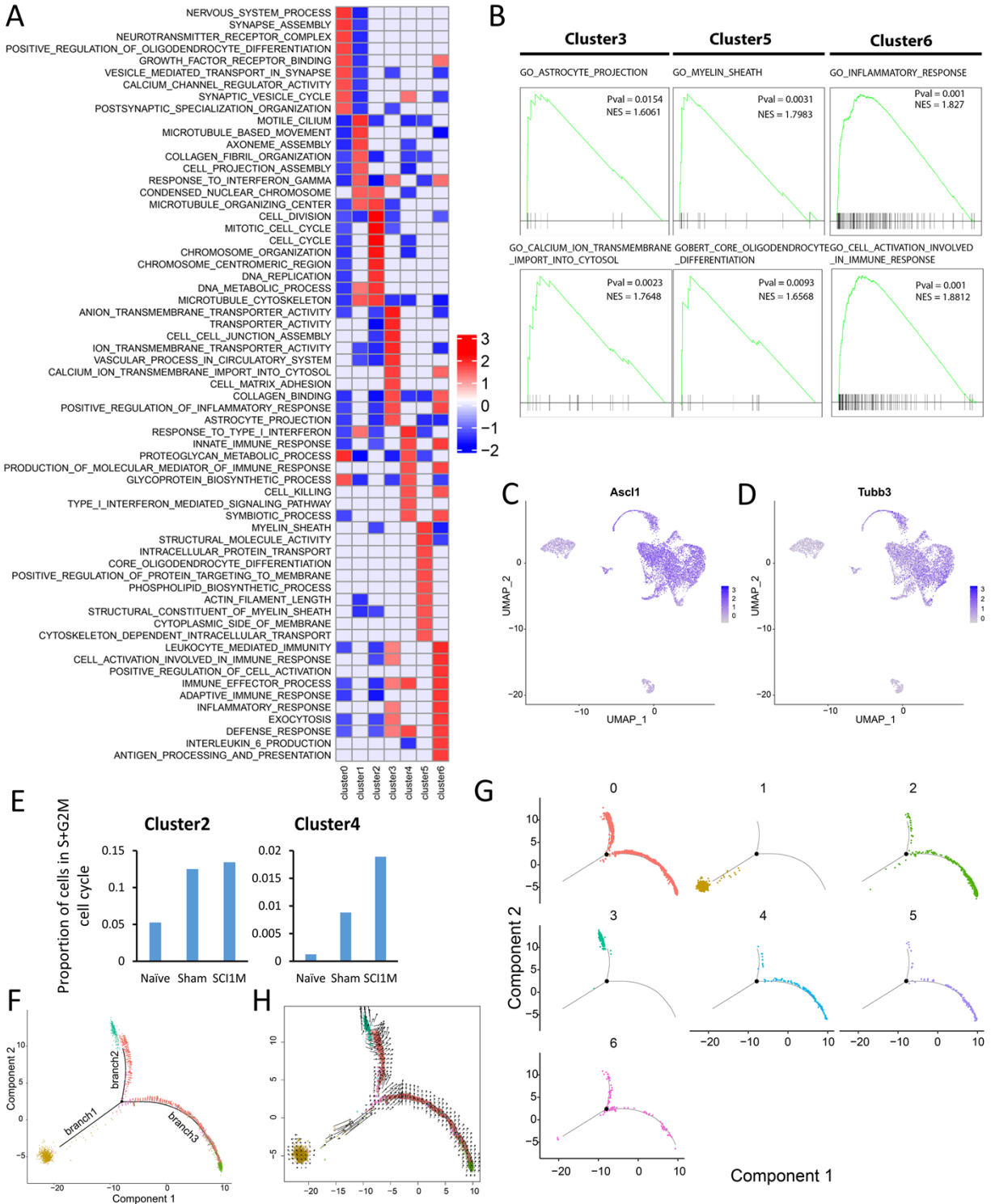


Figure S2. The gene set enrichment and trajectory analyses of astrocyte lineage subpopulations at sub-chronic SCI stage. Related to Figure 1. **(A)** The heatmap of gene set enriched in each cluster. **(B)** GSEA shows the enrichment of functions in Cluster3/5/6. **(C and D)** UMAP visualization showing neuronal marker expression: (*Ascl1*(C) and *Tubb3*(D)). **(E)** The proportion of cells in S and G2M phases with significant differences between Naïve, Sham and SCI1M samples according to an equality of proportions test using Pearson's chi-squared distribution. Cluster2 and

Cluster4 cells depicted significant ($p\text{-value} < 0.001$) differences. **(F and G)** Single-cell trajectory analysis of combined cells and cluster-specific cells throughout the three SCI conditions using Monocle2. Colors represent clusters identified. **(I)** The velocity results are shown on the two principal components calculated by monocle2.

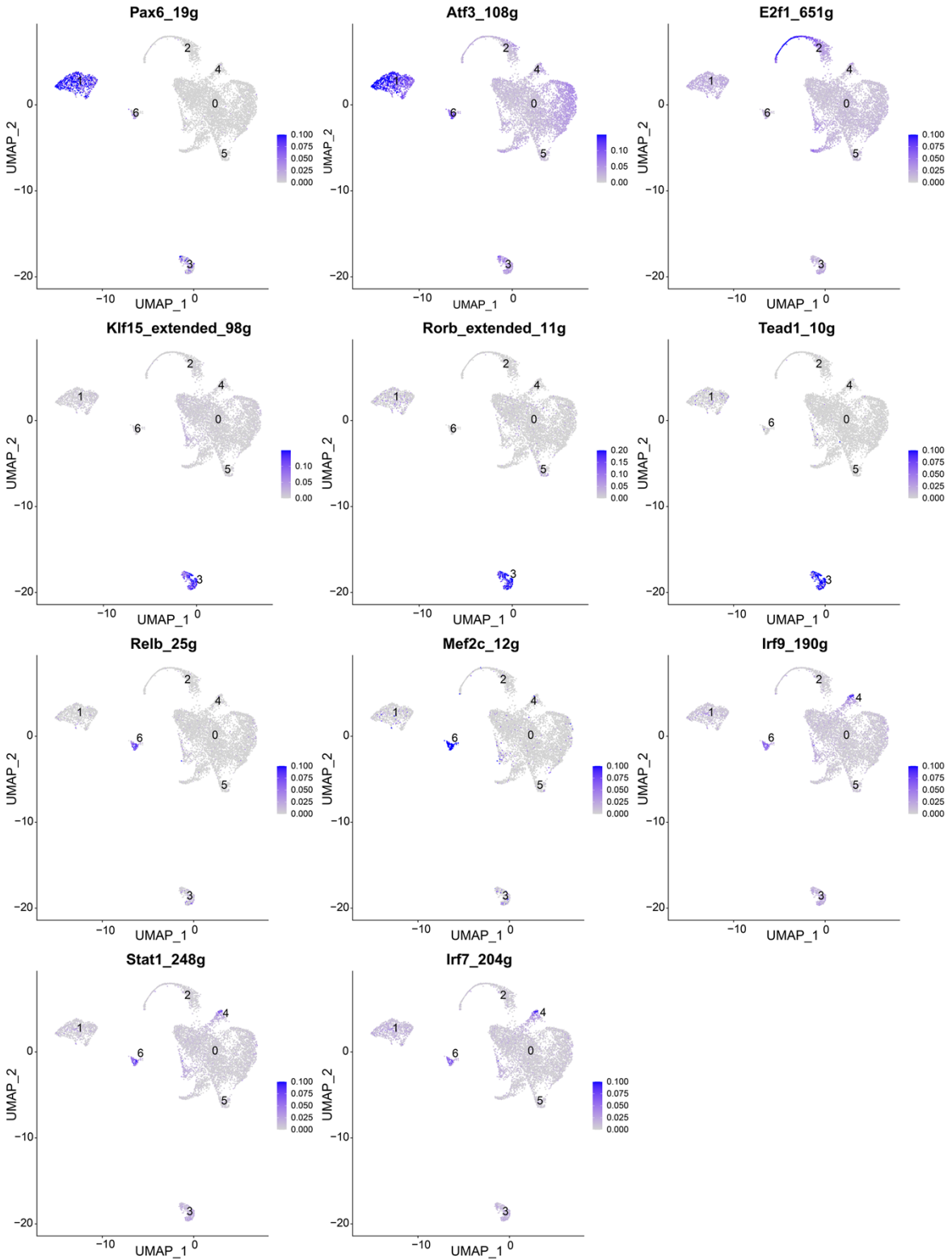


Figure S3. Regulon activity scores based on UMAP plots. Related to Figure 2. The activity of regulons in each cluster is identified by AUCell scores. Each dot is a cell and colored by blue means high AUCell scores.

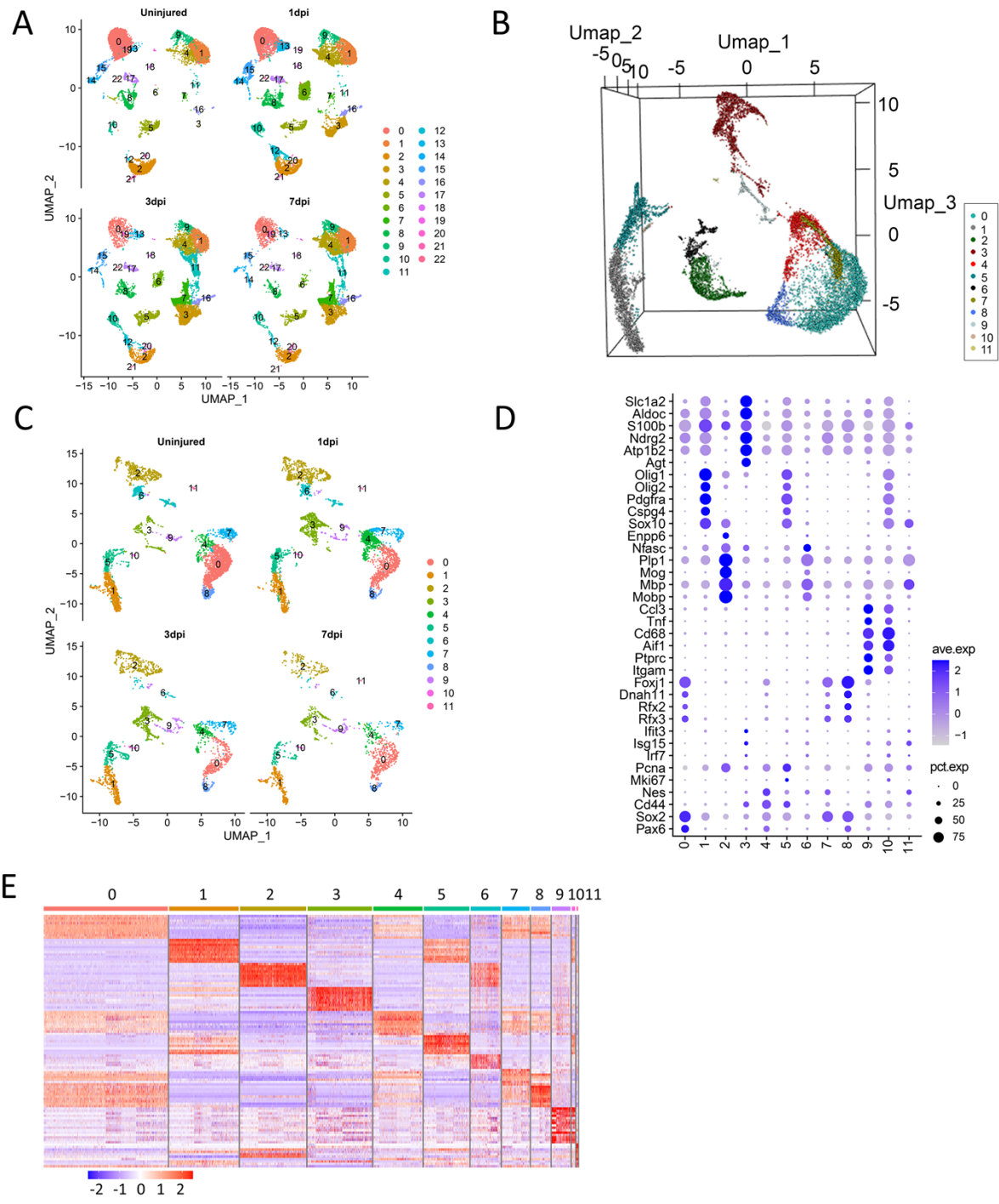
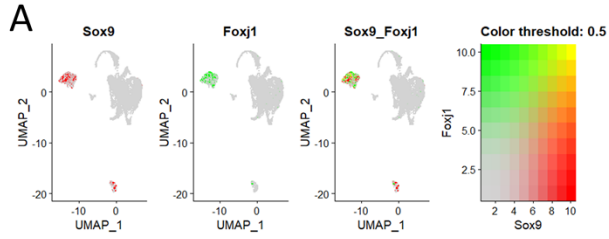
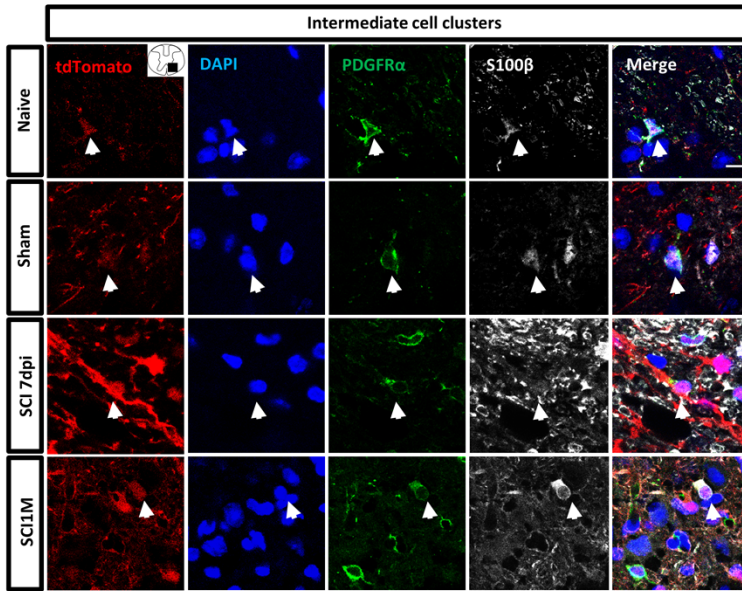


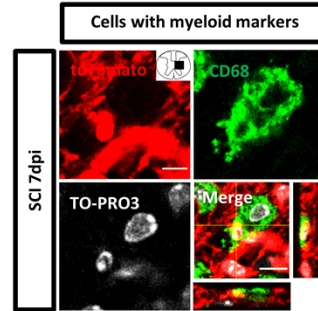
Figure S4. Identification of major cell types using cell marker expression signatures at acute SCI stage (GSE162610). Related to Figure 3. **(A)** UMAP of purified cells split by samples. **(B)** Three-dimensional UMAP visualization of astrocyte lineage cells. **(C)** UMAP of astrocyte lineage cells (defined by the presence of multiple astrocyte markers) split by samples. **(D)** Dot plot of expression levels of cell marker genes in the subpopulations. **(E)** Heatmap of top 10 differentially expressed genes (DEGs) in each cluster. Cluster numberings are the same for **(B-E)**, and the figure at http://jiaqianwulab.org/photoalbum/photo_thumbs/Acute_stage_3D_2.gif



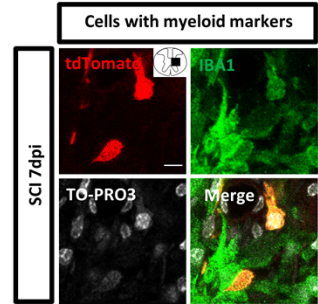
B



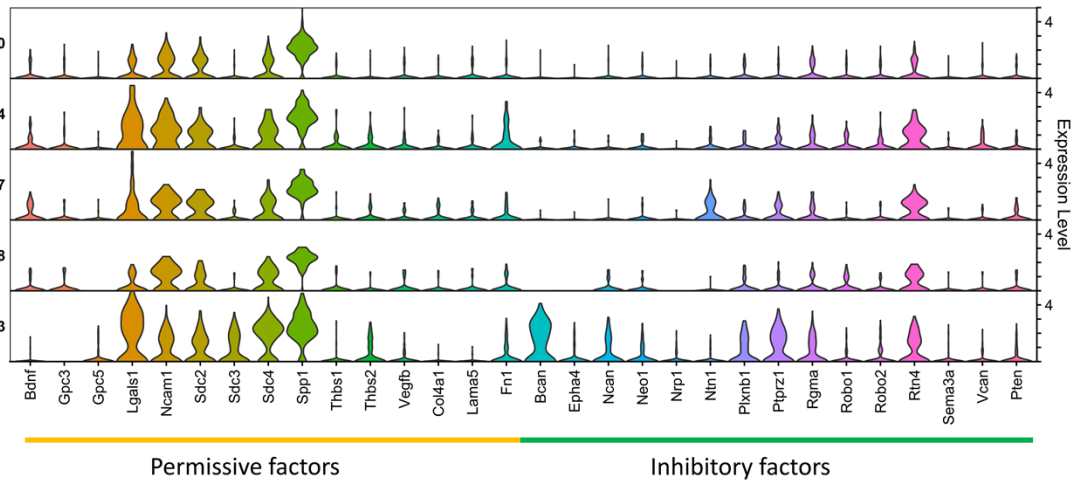
C



D



E



F

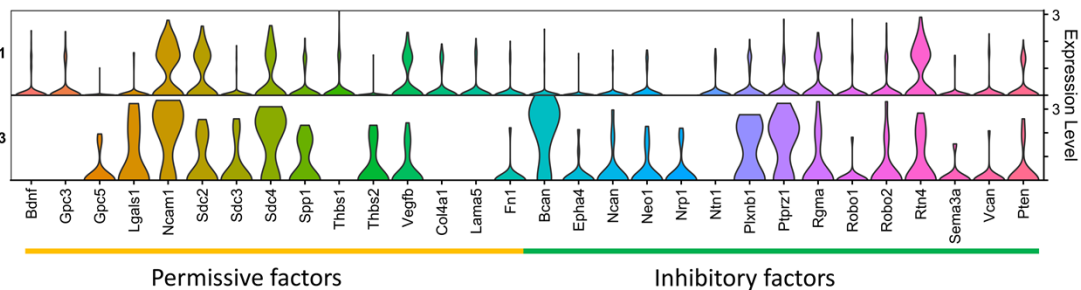


Figure S5. Immunohistochemical validation of intermediate cell subpopulations, and the expression patterns of permissive and inhibitor factors in astrocyte-ependymal and cells with only astrocyte markers. Related to Figure 4 and 5. **(A)** Co-expression of *Sox9*⁺/*Foxj1*⁺ in Cluster1 at sub-chronic stage. **(B)** Histological validation of the intermediate cell subpopulations using S100 β and PDGFR α staining in Naïve, Sham, SCI 7dpi and SCI1M in ventral horn at 600 μ m rostral from epicenter. White arrows represent the tdT⁺ cells (red) were co-localized with S100 β (white) and PDGFR α (green) immunostaining. Scale bar, 10 μ m. **(C-D)** Immunostaining of myeloid cell marker CD68 (green, **C**) and IBA1 (green, **D**) in tdT⁺ (red) cells at 7dpi (**C**, at epicenter; **D**, at 400 μ m caudal from the epicenter). Scale bar, 10 μ m. **(E)** The expression pattern of axon inhibitory factors and permissive factors in astrocyte-ependymal-Nes^{low} subpopulations (Cluster0/7/8), astrocyte-ependymal-Nes^{high} subpopulations (Cluster4) and the subpopulations with only astrocyte markers (Cluster3) at 7dpi. **(F)** The expression pattern of axon inhibitory factors and permissive factors in astrocyte-ependymal-Nes^{low} subpopulation (Cluster1) and the subpopulations with only astrocyte markers (Cluster3) at SCI1M.

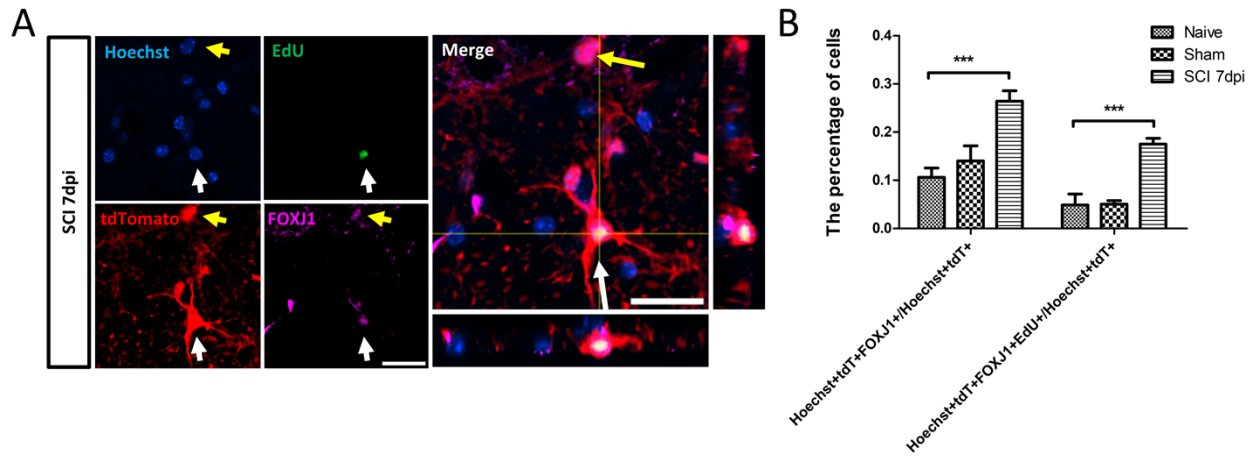


Figure S6. Quantitative assessments of astrocyte-ependymal cell proliferation in Naïve, Sham, and SCI 7dpi groups. Related to Figure 6 **(A)** Representative images from EdU labeling were taken in the ventral horn at 600-800 μm rostral to the epicenter. The white arrow indicates an EdU/tdT/FOXJ1 triple positive cell and the yellow arrow shows a tdT/FOXJ1 cell without EdU. Scale bar, 25 μm . **(B)** The proportion of astrocyte-ependymal and astrocyte-ependymal proliferation subpopulations among tdT+ cells. N=4 fields per group. The barplots (left) represents the percentage of Hoechst+/tdT+/FOXJ1+ cells out of all Hoechst+/tdT+ cells, while the barplots (right) represents the percentage of Hoechst+/tdT+/FOXJ1+/EdU cells out of all Hoechst+/tdT+ cells. Error bars depict standard error mean (SEM). Independent t-tests. *, $p < 0.05$; **, $p < 0.01$, ***, $p < 0.001$ compared with other groups.